ELSEVIER

# Porcine reproductive and respiratory syndrome virus induces apoptosis through a mitochondria-mediated pathway

Sang-Myeong Lee [a], Steven B. Kleiboeker [a,b,*]

[a] Department of Veterinary Pathobiology, College of Veterinary Medicine, University of Missouri-Columbia, USA
[b] Veterinary Medical Diagnostic Laboratory, College of Veterinary Medicine, University of Missouri-Columbia, USA

## Abstract

As with a number of other viruses, Porcine reproductive and respiratory syndrome virus (PRRSV) has been shown to induce apoptosis, although the mechanism(s) involved remain unknown. In this study we have characterized the apoptotic pathways activated by PRRSV infection. PRRSV-infected cells showed evidence of apoptosis including phosphatidylserine exposure, chromatin condensation, DNA fragmentation, caspase activation (including caspase-8, 9, 3), and PARP cleavage. DNA fragmentation was dependent on caspase activation but blocking apoptosis by a caspase inhibitor did not affect PRRSV replication. Upregulation of Bax expression by PRRSV infection was followed by disruption of the mitochondria transmembrane potential, resulting in cytochrome $c$ redistribution to the cytoplasm and subsequent caspase-9 activation. A crosstalk between the extrinsic and intrinsic pathways was demonstrated by dependency of caspase-9 activation on active caspase-8 and by Bid cleavage. Furthermore, in this study we provide evidence of the possible involvement of reactive oxygen species (ROS)-mediated oxidative stress in apoptosis induced by PRRSV. Our data indicated that cell death caused by PRRSV infection involves necrosis as well as apoptosis. In summary, these findings demonstrate mechanisms by which PRRSV induces apoptosis and will contribute to an enhanced understanding of PRRSV pathogenesis.
© 2007 Elsevier Inc. All rights reserved.

Keywords: PRRSV; Apoptosis; Caspase; Oxidative stress; Reactive oxygen species (ROS); Pathogenesis

## Introduction

There are two major types of cell death, necrosis and apoptosis, which differ both morphologically and biochemically. Necrosis is a passive (or accidental) cell death due to depletion of cellular resources and is characterized by increased ion permeability of the plasma membrane, cellular swelling and osmotic lysis followed by extensive tissue damage and an intense inflammatory response (Schwartz et al., 1993). On the other hand, apoptosis is described as an active (or programmed) cell death which is a cellular mechanism for suicide. Cells undergoing apoptosis show highly characteristic morphological changes, including shrinkage, blebbing of the plasma membrane, chromatin condensation and DNA fragmentation (Con-

nolly et al., 2000). DNA fragments are enclosed by apoptotic bodies, which are recognized and removed by phagocytes without provoking an inflammatory response. Biochemically, apoptotic cells are characterized by disruption of the mitochondrial transmembrane potential, externalization of phosphatidylserine in the outer leaflet of the plasma membrane, selective proteolysis of a subset of cellular proteins, and cleavage of chromosomal DNA into internucleosomal fragments.

Apoptosis can be induced by two major pathways, the extrinsic and intrinsic pathways, both of which are regulated by caspases. Caspases, a family of cysteine proteases, exist as inactive proenzymes and are activated after cleavage at specific aspartate residues upon apoptotic signals. Cleaved caspases activate other caspases by proteolysis (Kidd, 1998). The extrinsic pathway is mediated by activation of caspase-8 that is initiated mainly by binding of death receptors to their ligands. Internal signals such as DNA damage, radiation, growth factor deprivation, viral infection, and chemotherapeutic agents trigger

* Corresponding author. ViraCor Laboratories, 1210 NE Windsor Dr., Lee's Summit, MO 64086, USA. Fax: +1 816 347 0143.
E-mail address: skleiboeker@viracor.com (S.B. Kleiboeker).

the intrinsic pathway, which involves the release of cytochrome $c$ from mitochondria. Subsequently, cytochrome $c$ binds to the adaptor molecule Apaf-1 (apoptotic protease activating factor-1) causing autocleavage of caspase-9 (Chu et al., 2001). These two pathways converge at the activation of executioner caspases (caspase-3, -6, and -7), which are responsible for the characteristic morphological changes of apoptosis (Budihardjo et al., 1999). The main targets of these caspases include DNA fragmentation factor (DFF) and poly (ADP-ribose) polymerase (PARP). A crosstalk exists between the extrinsic and intrinsic pathways. Activated caspase-8 mediates the cleavage of Bid to truncated Bid (tBid), an active form. tBid translocates to mitochondria and activates the intrinsic pathway via the release of cytochrome $c$ (Li et al., 1998).

Apoptosis plays an essential role in development and maintenance of homeostasis in multicellular organisms. More-over, apoptosis also plays a crucial role in the pathogenesis of several viral infections (Rudin and Thompson, 1997). Apoptosis is often considered as an innate defense mechanism that limits virus infection by elimination of infected cells (Everett and McFadden, 1999). Therefore, many viruses inhibit apoptosis to prevent premature cell death and thus increase progeny viral production. However, some viruses induce apoptosis to enhance progeny viral transmission and avoid the immune response (Thomson, 2001). Many studies have demonstrated that PRRSV induces apoptosis both *in vitro* and *in vivo* (Choi and Chae, 2002; Kim et al., 2002; Labarque et al., 2003; Miller and Fox, 2004; Sirinarumitr et al., 1998; Suarez et al., 1996; Sur et al., 1997, 1998). PRRSV infection of both MARC-145 cells and porcine alveolar macrophages (PAM) resulted in apoptosis characterized by morphological changes and DNA fragmentation. However, it is controversial whether PRRSV induces apoptosis directly (in infected cells) or indirectly (in bystander cells). There is evidence of direct induction of apoptosis by PRRSV. For example, GP5 (ORF5) of PRRSV has been shown to be an apoptosis inducer (Gagnon et al., 2003; Suarez et al., 1996). However, cells stably expressing GP5 did not show any characteristics of apoptosis (Lee et al., 2004). A nontypical apoptosis was characterized by double staining of DNA fragmentation and PRRSV N protein in unattached dead cells (Kim et al., 2002). However, other studies have shown that PRRSV induces apoptosis mostly in uninfected bystander cells both *in vitro* and *in vivo*. In previous studies, the majority of apoptotic cells in lung lavages, lungs, and lymphoid tissues were not positive for PRRSV infection (Choi and Chae, 2002; Kim et al., 2002; Labarque et al., 2003; Miller and Fox, 2004; Sirinarumitr et al., 1998; Suarez et al.,

1996; Sur et al., 1997, 1998). Chang et al. reported that alveolar macrophages from PRRSV-infected pigs showed a significantly increased apoptotic rate (22–34%) compared to porcine circovirus 2 infected alveolar macrophages (3%) (Chang et al., 2005). Given the fact that only 5–10% of alveolar macrophages were PRRSV-infected, these authors suggested that TNF-α or GP5 released from PRRSV-infected cells caused apoptosis in bystander cells. Another study from the same group demonstrated that increased FasL expression in PRRSV-infected macrophages caused apoptosis in co-cultured swine splenic lymphocytes (Chang et al., 2007). Based on these results, the majority of apoptotic cells could be non-infected bystander cells although PRRSV induces apoptosis in virus-infected macrophages and dendritic cells. To conclusively prove this, further comprehensive studies which investigate early apoptotic processes are required. Most of the previous studies measured DNA fragmentation by a TUNEL assay, a technique that cannot detect early biochemical changes in apoptotic cell and also cannot differentiate late apoptosis versus necrosis. In the present study we provide further evidence of apoptosis induced by PRRSV directly in PRRSV-infected cells. In addition the pathway through which PRRSV infection induces apoptosis in a continuous cell line is demonstrated.

## Results

### PRRSV replication in MARC-145 cells and its effect on cell viability and morphology

Prior to evaluating the characteristics of apoptosis induced by PRRSV, PRRSV replication and cell viability were determined. When PRRSV was innoculated at MOI = 0.1, virus replication reached the highest level (over 6 $\log_{10}$ TCID$_{50}$/ml) at 48 h p.i., which was followed by a slight decline at 60 h p.i. (Fig. 1A). As shown in Fig. 1B, following PRRSV infection, cell viability dropped gradually to 92% during the first 48 h and then decreased further to 89% at 60 h p.i. Corresponding morphological changes in the cells are shown in Fig. 1C. Typical PRRSV-induced cytopathic effect (CPE) characterized by cellular rounding and clumping was visible at 48 and 60 h p.i. The percentage of PRRSV-infected cells was determined by flow cytometric analysis of nucleocapsid protein expression (Fig. 1D). The majority of cells (over 80%) were positive for viral protein at 48 and 60 h p.i., time points which showed a characteristic CPE in PRRSV-infected cells.

Fig. 1. Infection of MARC-145 cells with PRRSV. (A) MARC-145 cells were infected with PRRSV at MOI = 0.1 and cell culture medium was collected at the indicated time points p.i, with each time point represented by triplicate samples. Samples were frozen −80 °C and thawed one time, and infectious virus titers were analyzed in MARC-145 cells using the Reed and Muench method (Reed and Muench, 1938). Values are shown as the mean ± SD from triplicate wells, and this experiment was repeated twice with consistent results. (B) Cell viability of mock or PRRSV-infected MARC-145 cells were determined at 24, 48, and 60 h p.i. using trypan blue exclusion assay. Values are shown as the mean ± SD from triplicate wells, and this experiment was repeated twice with consistent results. (C) PRRSV-infected MARC-145 cells were fixed in methanol 24, 48, and 60 h p.i. and observed under phase contrast microscope. (D) PRRSV-infected MARC-145 cells were harvested at 24, 48, and 60 h p.i. and fixed with 2% PFA and permeabilized with 70% ethanol. After washing with PBS, cells were stained with SDOW-17 antibody against the PRRSV nucleocapsid protein followed by anti-mouse-FITC conjugate. FITC positive cells were analyzed by flow cytometry in the FL-1 channel. X-axis represents $\log_{10}$ fluorescent intensity and Y axis shows cell counts. *; $P < 0.001$ compared to mock-infected cells at the same time point.

*PRRSV infection induces chromatin condensation, DNA fragmentation, and PS exposure*

General characteristics of apoptotic cells were evaluated in PRRSV-infected cells. Annexin V has a high affinity for the phospholipid phosphatidylserine (PS) which is translocated from the inner leaflet of the plasma membrane to the outer leaflet during the early stages of apoptosis. As shown in Fig. 2A, PRRSV-infected cells show very little staining above that of the uninfected control cells at 24 h p.i. However, at 48 and 60 h
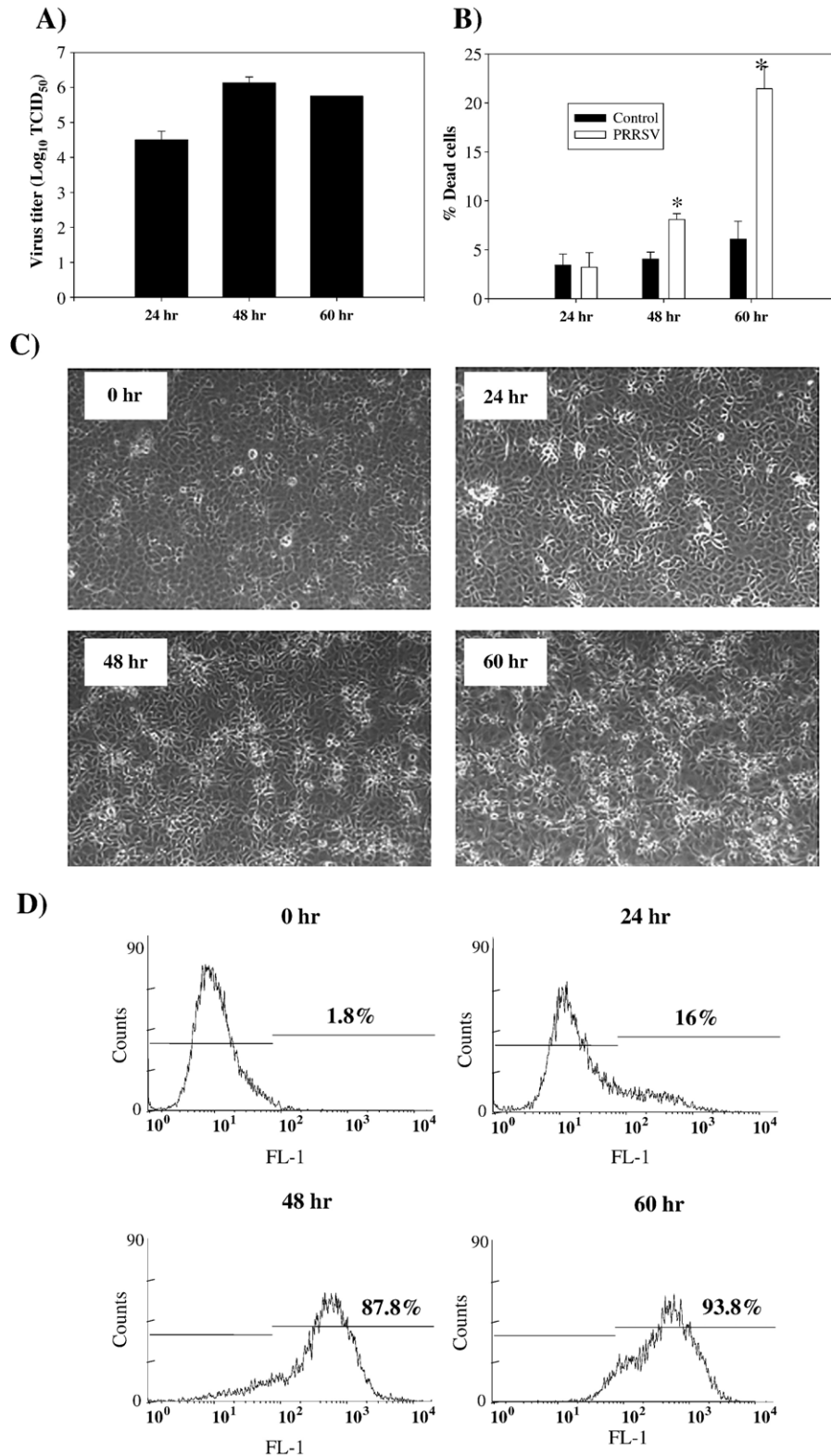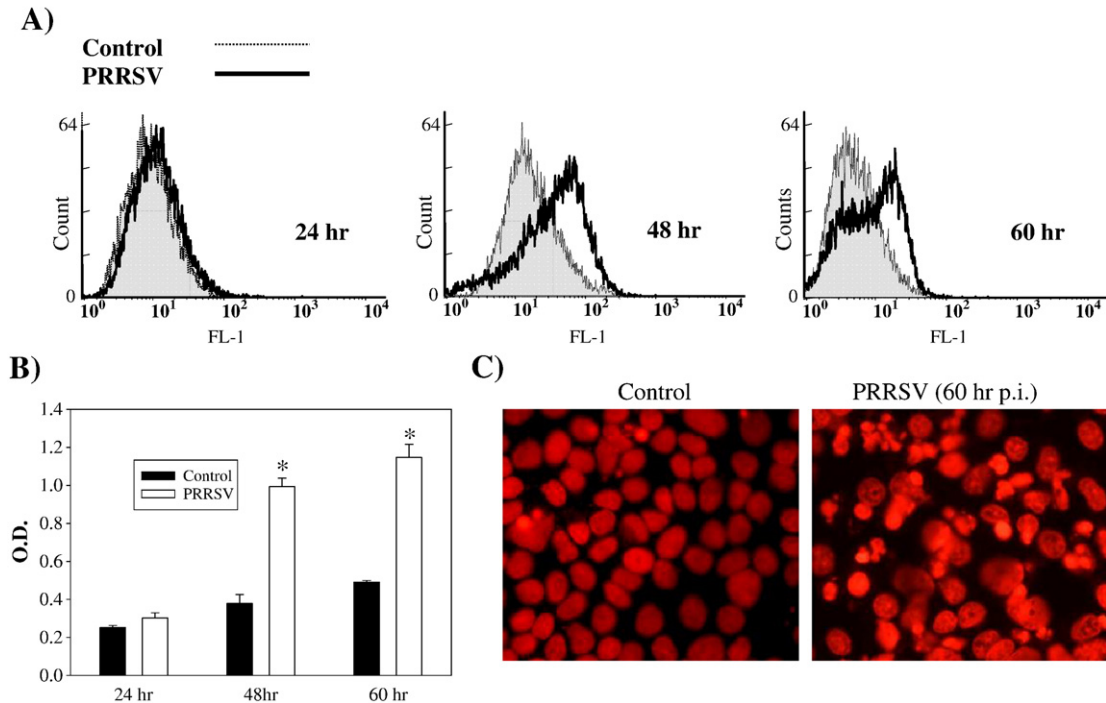
Fig. 2. Apoptosis in PRRSV-infected cells. (A) Adherent cells were harvested by trypsin treatment and combined with floating cells. Then cells were stained with annexin V–flour staining kit followed by flow cytometry analysis. (B) Cells infected with PRRSV were lysed at 24, 48, and 60 h p.i. DNA fragments in cell lysates were quantitatively measured using the DNA fragmentation ELISA. Values are shown as the mean±SD of the optical density (O.D.) values from duplicate wells, and these results are representative of three independent experiments. (C) Chromatin condensation was visualized in MARC-145 cells fixed with ice-cold methanol and stained with PI solution containing RNaseA. *; $P < 0.001$ compared to mock-infected cells at the same time point.

p.i., the median expression of green fluorescence was 13.31% in control cells and 31.34% in PRRSV-infected cells, indicating the extensive staining for annexin V in virus-infected cells. DNA fragmentation, which detects a late apoptotic process, was also determined. The amount of DNA fragmentation in the cytoplasm of PRRSV-infected cells was not different from mock-infected cells at 24 h p.i. but significantly increased at 48 h and 60 h p.i. as PRRSV replication progressed (Fig. 2B). In addition to biochemical changes, nuclear morphological change was studied by staining with propidium iodide, a fluorescent DNA intercalator. Infection with PRRSV caused distinct changes in nuclear morphology such as chromatin condensation and nuclear segments in apoptotic bodies as shown in Fig. 2C. Collectively, PRRSV-infected cells displayed characteristics of apoptosis such as annexin V staining, DNA fragmentation, chromatin condensation, and apoptotic bodies.

*PRRSV infection activates caspase cascades*

Caspases are activated exclusively in apoptosis but not in necrosis (Cryns and Yuan, 1998). Therefore, to further confirm that PRRSV induces apoptosis and to characterize the apoptotic pathways activated by PRRSV, total caspase activity was first determined. MARC-145 cells were uninfected or infected with PRRSV for 24, 48, or 60 h and attached cells as well as non-attached cells were harvested. Activated caspases were labeled by FITC-conjugated z-VAD-FMK irreversibly and were analyzed by flow cytometry (Fig. 3). Following PRRSV infection, cells with activated caspases represented 11.1%, 30.57%, and

43.23% of the total cell population at 24, 48, and 60 h p.i., respectively, while control cells stained for activated caspases ranged from 6.7% to 9.2% (Figs. 3A–C). To differentiate the two apoptotic pathways, intrinsic and extrinsic, it was determined which initiator caspase (caspase-8 or caspase-9) was activated in PRRSV-infected cells. Caspase activity was measured using a colorimetric method that detects hydrolysis of a synthetic substrate IETD-pNA for caspase-8 and LEHD-pNA for caspase-9. Following PRRSV infection, caspase-8 activity started to increase at 48 h p.i., and the activity was more than two-fold higher compared to control cells at 60 h p.i. (Fig. 3D). A similar pattern was seen in caspase-9 activity. The initial caspase-9 activation at 48 h p.i. was followed by a significant increase at 60 h p.i. (Fig. 3E). Signal cascades activated by these two caspases converge on caspase-3 which is one of executioner caspases. Therefore, caspase-3 activity was also measured using a specific substrate, DEVD-pNA. As shown in Fig. 3F, this caspase was also activated by PRRSV infection. The level of caspase-3 activity was about 2.5-fold and 4.0-fold higher at 48 and 60 h p.i., respectively, compared to uninfected control cells. Taken together, these results demonstrate that PRRSV triggers caspase-8, -9, and -3 activation.

*PRRSV infection triggers PARP cleavage which is caspase-dependent*

PARP is a substrate for activated caspase-3 and cleaved PARP is considered a hallmark of apoptosis. To provide additional evidence of caspase activation and apoptosis induced
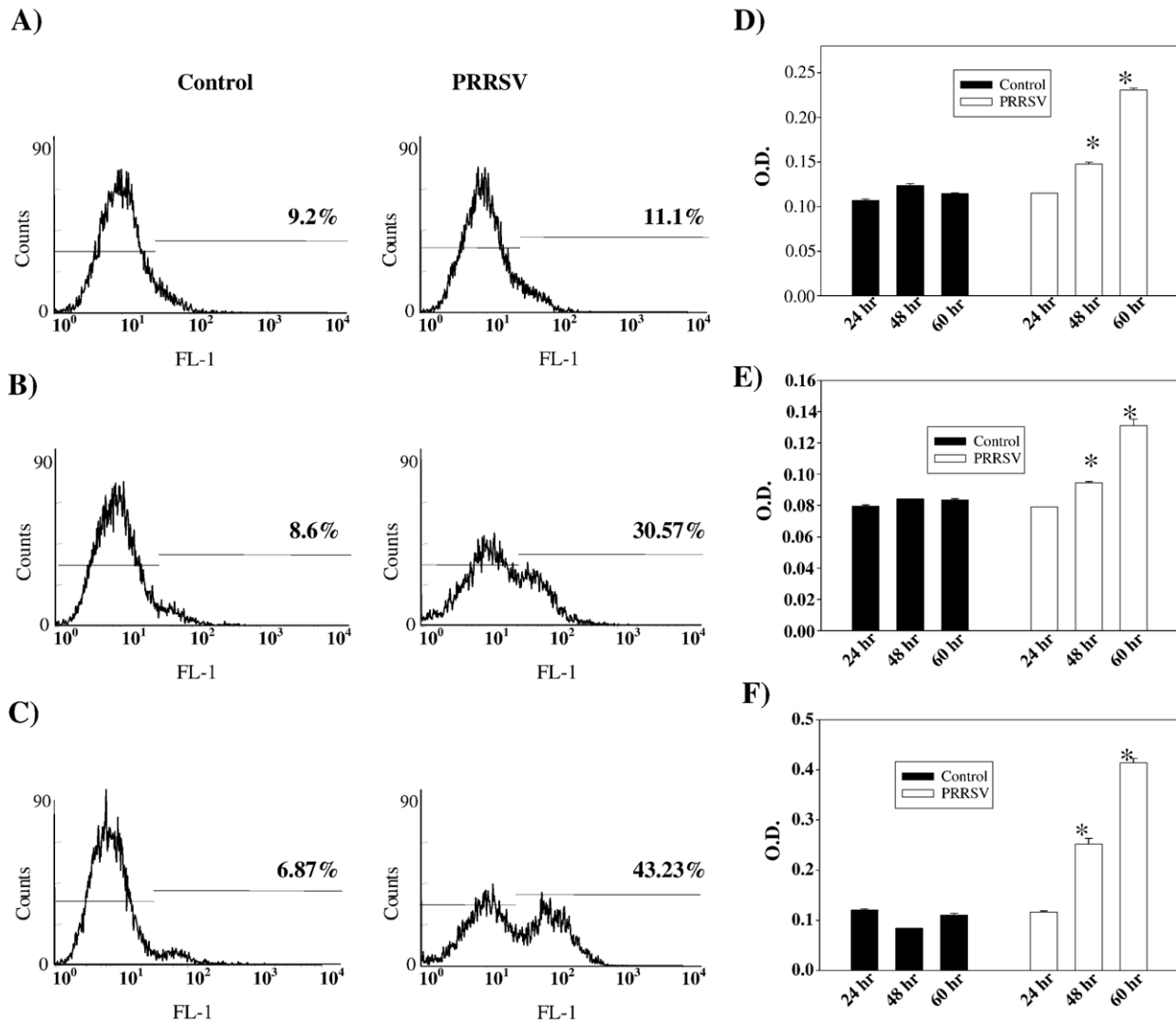
Fig. 3. PRRSV infection activates caspases. Both adherent and floating cells were labeled with FITC-conjugated z-VAD-FMK at 24 h (A), 48 h (B), and 60 h (C) p.i. as described in Materials and methods. The percentage of positive cells is indicated in each panel. These results are representative of three independent experiments. Caspase-8 (D), caspase-9 (E), and caspase-3 (F) activities of mock or PRRSV-infected cells were determined at the indicated times p.i. Cytoplasmic extracts from both adherent and floating cells were prepared and analyzed for each caspase activity using a colorimetric assay with specific substrate for each caspase. Results are expressed as O.D. values from 100 μg of protein. ELISAs were performed in triplicate, and values are shown as mean±SD. These results are representative of at least three independent experiments. *; $P < 0.05$ compared to mock-infected cells at the same point.

by PRRSV, PARP cleavage was monitored during PRRSV infection. As shown in Fig. 4A, PRRSV infection significantly increased levels of cleaved PARP at 48 h p.i., and this level was further increased at 60 h p.i. The pattern of cleaved PARP appearance was similar to that of caspase activation. In uninfected control cells, the amount of cleaved PARP remained relatively stable at low levels. Further experiments using z-VAD-FMK, a broad spectrum caspase inhibitor, determined that PARP cleavage was caspase-dependent. When PRRSV-infected cells were treated with z-VAD-FMK at different concentrations, the amount of cleaved PARP was significantly reduced in dose-dependent manner and cleaved product was not detectable following treatment with 100 and 200 μM concentrations (Fig. 4A). To determine the involvement of the two apoptotic pathways in PARP cleavage, caspase-8 and caspase-9 were inhibited with the cell permeable, irreversible, specific caspase

inhibitors z-IETD-FMK and z-LEHD-FMK, respectively. When cells infected with PRRSV were treated with caspase inhibitor at 5, 10 and 20 μM, both caspase inhibitors significantly decreased PRRSV-induced PARP cleavage. At the highest concentrations of z-IETD-FMK and z-LEHD-FMK, cleaved PARP was undetectable in PRRSV-infected cells (Fig. 4A). These findings indicate that, in MARC-145 cells, PRRSV may induce apoptosis through both caspase-8 and caspase-9 dependent pathways. The implication is that the death-receptor-mediated extrinsic pathway and mitochondrial-mediated intrinsic pathway are both activated and there is significant crosstalk between the two pathways, which means that tBid transmits signals from the extrinsic (caspase-8) to the intrinsic pathway (caspase-9) in PRRSV-induced apoptosis (Roy and Nicholson, 2000).

In additional experiments, it was determined if PRRSV-induced DNA fragmentation was caspase-dependent. A broad
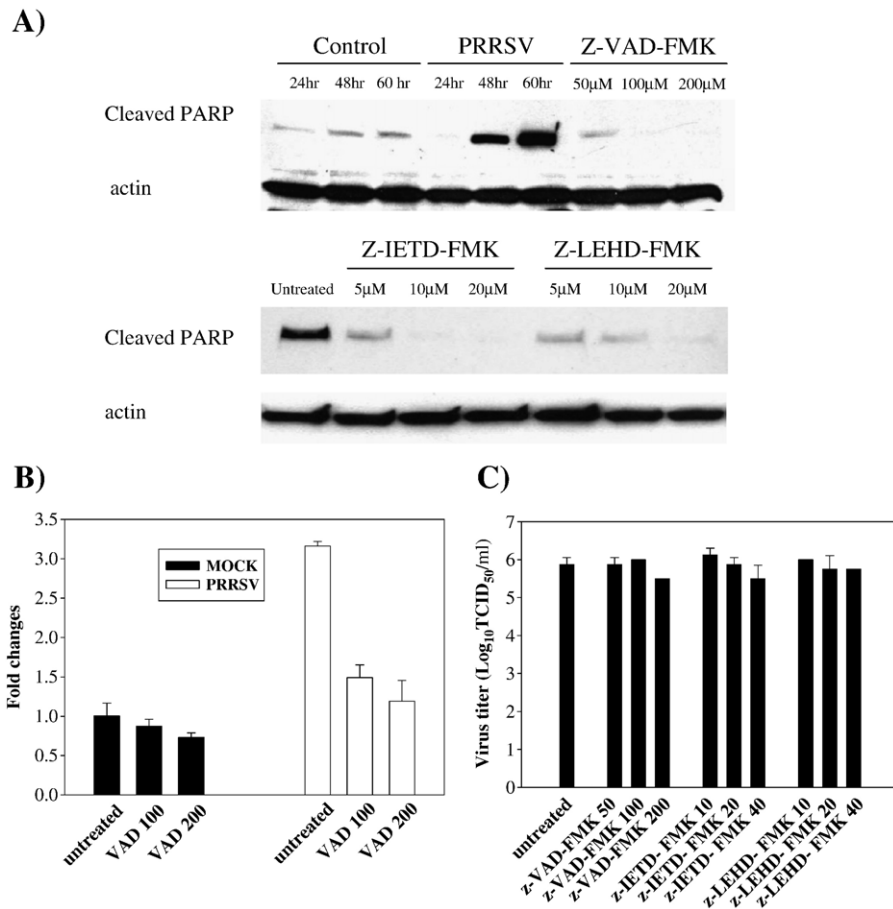
Fig. 4. PRRSV triggered PARP cleavage and DNA fragmentation which were caspase-dependent. (A) The level of cleaved PARP was monitored by Western blot. Cells were infected with PRRSV and treated with caspase inhibitors, z-VAD-FMK, z-IETD-FMK, and z-LEHD-FMK. Whole cell extracts from both adherent and floating cells were then prepared at 24, 48, or 60 h p.i. for untreated cells and 60 h p.i. for caspase-inhibitor-treated cells and immunoblotted with cleavage site specific anti-PARP polyclonal antibody. A representative result from three independent experiments is shown. Following infection, cells were treated with z-VAD-FMK and the DNA fragmentation ELISA was performed with cytoplasmic extracts (B) from indicated time points p.i. These results are representative of at least three independent experiments. *; $P < 0.001$ compared to untreated PRRSV-infected cells. (C) Infectious virus titers in cell culture medium were determined at 60 h p.i. and virus titers are shown as $\log_{10}$ TCID$_{50}$/ml. All experiments were repeated three times with similar results.

spectrum caspase inhibitor, z-VAD-FMK, was used at 100 μM and 200 μM to block caspase activation. DNA fragmentation in PRRSV-infected cells was reduced more than 50% with caspase inhibitor treatment (Fig. 4B). This result, as well as caspase-dependent PARP cleavage, suggests that PRRSV induces apoptosis by caspase-dependent mechanisms.

To determine the role of apoptosis in PRRSV infection, virus progeny release in the presence or absence of the caspase inhibitor z-VAD-FMK, z-IETD-FMK, and z-LEHD-FMK was determined by measuring the 50% tissue culture infectious dose (TCID$_{50}$) from cell culture supernatants. These infection studies revealed that none of three caspase inhibitors significantly affected viral replication (Fig. 4C). This demonstrates that apoptosis induction may not play a major role in PRRSV replication *in vitro*.

*Crosstalk between intrinsic and extrinsic pathway may exist in PRRSV-infected cells*

The results presented here demonstrated that PRRSV infection activates both caspase-8 and caspase-9 mediated apoptosis

pathways. The observation that caspase-8 is activated in PRRSV-infected cells led us to test the involvement of the TNF receptor superfamily. For that purpose, cell surface expression of TNFR1, Trail, and FasL was determined by IFA at 60 h PI. Results are shown in Fig. 5. Enhanced expression of TNFR1 and FasL was evident on the cell surface of PRRSV-infected cells. In this experiment, cells were not co-stained with anti-PRRSV antibody because antibodies available for anti-PRRSV staining require permeabilization for intracellular staining. At 60 h PI, about 94% of cells stained for nucleocapsid protein of PRRSV (Fig. 1D). Therefore, we concluded that most of cells with upregulated TNFR1 or FasL are PRRSV-infected cells. When MARC-145 cells are infected with PRRSV, typical CPE includes cellular rounding and clumping which are likely responsible for clusters or foci of TNFR1 or FasL positive cells for PRRSV-infected image shown in Fig. 5. However, the expression of Trail was not increased in infected cells or more likely decreased in some cells in this population. Therefore, these findings suggest that PRRSV upregulates the cell surface expression of TNFR1 and FasL, but not Trail, implying a
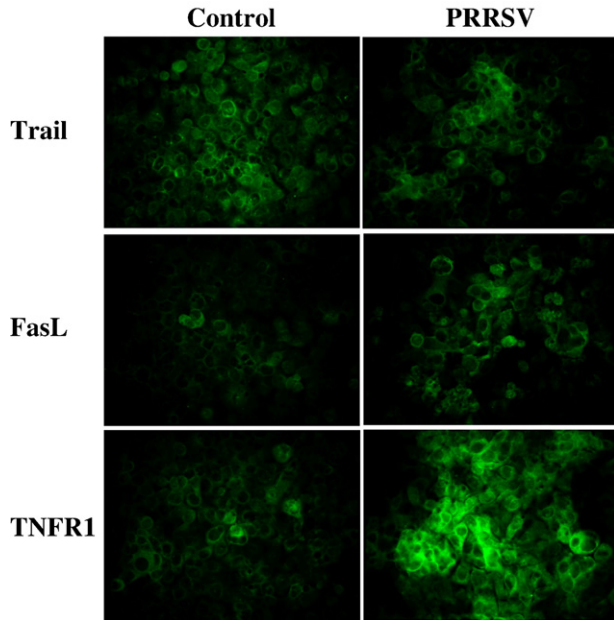
Fig. 5. PRRSV increases cell surface expression of TNFR1 and FasL but not Trail. Cells were fixed and stained for TNFR1, Trail, and FasL at 60 h p.i. and observed under by fluorescence microscopy.

possible role of these molecules in apoptosis of PRRSV-infected cells.

In subsequent experiments, it was determined if there was crosstalk between the two pathways. It has been shown that death-receptor-mediated activation of caspase-8 cleaves Bid, a Bcl-2 family member. Cleaved Bid then facilitates mitochondria-mediated caspase-9 activation. Therefore, to test this possibility in PRRSV-induced apoptosis, we determined if blocking caspase-8 activity affects caspase-9 activation. Following z-IETD-FMK treatment at 20 μM, the level of caspase-9 activity in PRRSV-infected cells declined to the level of uninfected control cells (Fig. 6A). Next it was determined if Bid was cleaved upon PRRSV infection. Western blot analysis revealed that tBid was not detected in uninfected cells but that PRRSV infection resulted in cleavage of the full-length 22 kDa Bid to 15 kDa tBid at 48 and 60 h p.i., possibly by activated caspase-8 (Fig. 6B). These results imply that the apoptosis signal cascade from the TNF receptor superfamily is transmitted to caspase-8 which in turn cleaves Bid. Cleaved Bid activates caspase-9, which links the extrinsic and intrinsic pathways.

### PRRSV infection disrupts mitochondria transmembrane potential and infection induces cytochrome c release from mitochondria

The Bcl-2 family includes a number of pro-apoptotic and anti-apoptotic proteins which are known to regulate apoptosis at the level of the mitochondria by changing relative levels. Therefore, levels of the major anti-apoptotic protein, Bcl-2, and the major pro-apoptotic protein, Bax, were visualized by IFA as shown in Fig. 7A, which demonstrates the qualitative differences in protein expression levels of Bcl-2 and Bax in uninfected cells versus PRRSV-infected cells. In mock-infected

control cells, bright staining of Bcl-2 was detected but Bax was undetectable. In contrast, after PRRSV infection for 60 h, the level of Bcl-2 was noticeably reduced while Bax expression was enhanced, implying that the ratio of Bcl-2/Bax was decreased by PRRSV infection. Thus, it is likely that pro-apoptotic signal is predominant over anti-apoptotic signal.

Next, it was determined if changes in mitochondrial transmenbrane potential ($\Delta\psi_m$) occurred in PRRSV-infected cells. MARC-145 cells were mock-infected or infected with PRRSV, and cells were harvested at indicated time points and assessed for $\Delta\psi_m$ using the MitoCapture assay. MitoCapture reagent selectively enters healthy polarized mitochondria and aggregates, resulting in a change of color from green to red. In apoptotic cells which have disrupted mitochondria membrane potential, MitoCapture is not able to penetrate mitochondria, and the monomeric form of MitoCapture fluoresces green. Therefore, using the MitoCapture reagent, live cells with low mitochondria membrane potential can be detected. Green fluorescence for each cell was measured using flow cytometry. Representative histograms of the green fluorescence intensity are shown in Fig. 7B. In PRRSV-infected cells, a slight decrease of mitochondria membrane potential was detected at 24 h p.i. mitochondria membrane potential was significantly disrupted at 48 and 60 h p.i., and the median expression of green fluorescence was 2.7-fold and 3.7-fold higher, respectively, in
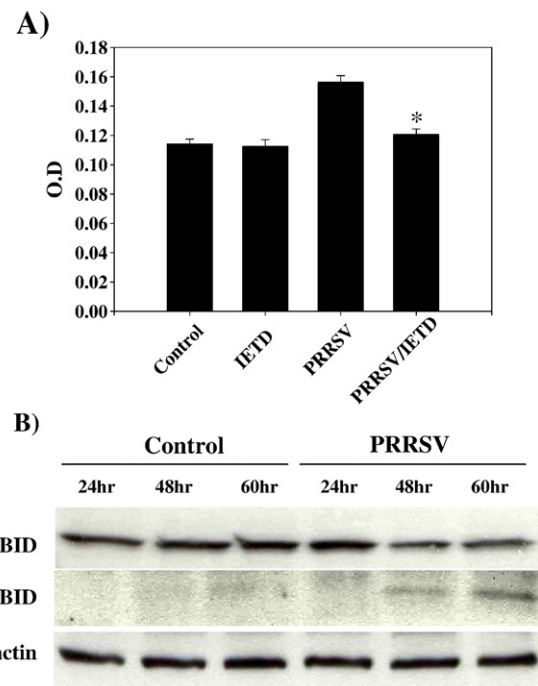


Fig. 6. Caspase-9 activity is dependent on caspase-8 activation and tBID expression is increased in PRRSV-infected cells. (A) Cells were infected with PRRSV and treated with the caspase-8 inhibitor, z-IETD-FMK at 20 μM. Adherent cells were harvested by trypsin treatment and combined with floating cells. Caspase-9 activity was measured using a colorimetric assay with a specific substrate. Values are shown as the means ± SD from triplicate wells and represent two independent experiments. (B) Cell lysates from both adherent and floating cells at different time points after PRRSV infection were immunoblotted and truncated BID was detected. This experiment was repeated two times with similar results. *; $P < 0.001$ compared to untreated PRRSV-infected cells.
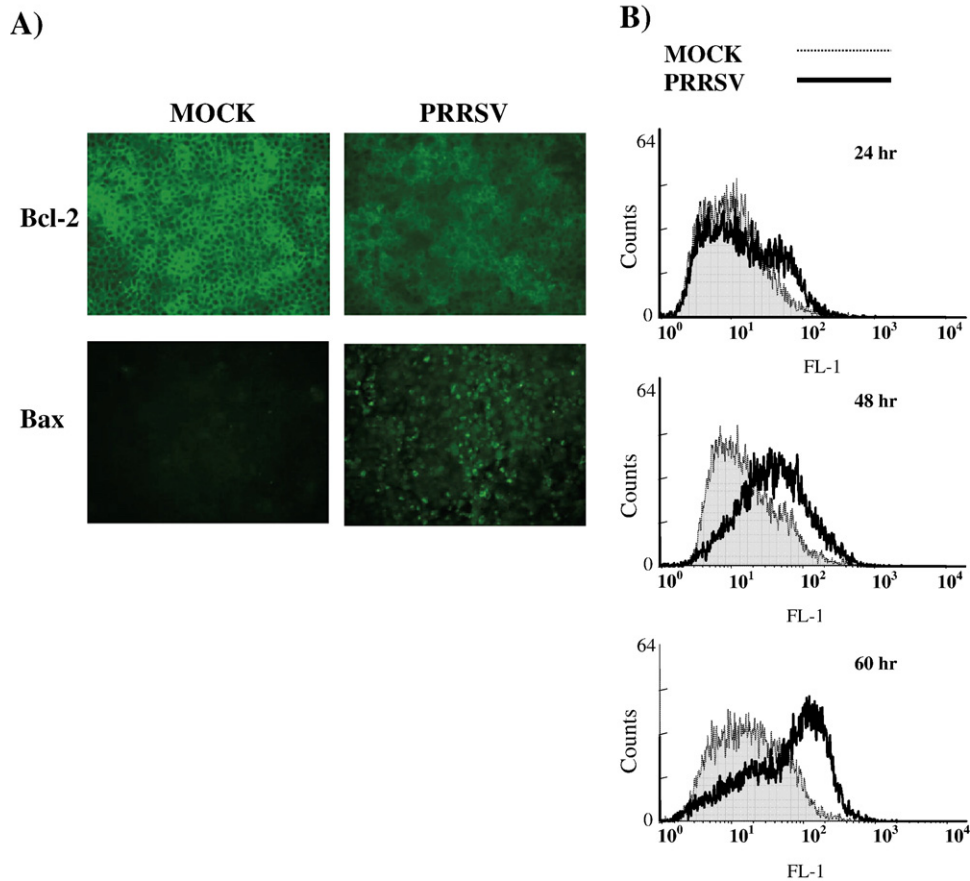
Fig. 7. Effect of PRRSV infection on Bcl-2 and Bax expression and on mitochondrial transmembrane potential. (A) Cells infected with PRRSV were fixed and permeabilized at 60 h p.i. and then stained for Bcl-2 and Bax. Slides were observed by fluorescence microscopy. (B) Cells infected with PRRSV (both adherent and floating cells) were collected and examined for disruption of mitochondrial transmembrane potential by using the fluorescent probe MitoCapture. MitoCapture-labeled cells were analyzed by flow cytometry.

virus-infected cells in comparison to the corresponding control cells.

Damaged mitochondria release pro-apoptotic factors, such as cytochrome $c$, which induce subsequent activation of caspase-9. Therefore, the distribution of cytochrome $c$ was determined. Fig. 8A shows the kinetics of cytochrome $c$ efflux from the mitochondria by immunoblotting of mitochondrial extracts and cytoplasmic extracts. Following PRRSV infection, increased cytochrome $c$ levels in cytoplasm were visible at 48 and 60 h p.i. (Fig. 8A). To further confirm this result, IFA was performed using monoclonal antibody against cytochrome $c$. As revealed by diffused staining in Fig. 8B, cytochrome $c$ was redistributed from mitochondria to the cytoplasm in a majority of the PRRSV-infected cells whereas in uninfected cells, cytochrome $c$ was present exclusively in the perinuclear zone, presumably associated with mitochondria.

*ROS contributes to the apoptotic process in PRRSV-infected cells*

In our previous studies, PRRSV increased ROS production and oxidative stress induced by ROS is also known as a mediator of apoptosis (Lee and Kleiboeker, 2005). Thus, the role of ROS in PRRSV-induced apoptosis was studied. The production of ROS was suppressed by three different antioxidants, PDTC, NAC and rotenone (RTN), at various concentrations. Importantly, the three antioxidants used in these experiments did not show cytotoxicity at all concentrations used. The level of apoptosis was evaluated by immunoblotting of cleaved PARP and measuring DNA fragmentation. As shown in Fig. 9A, all antioxidants prevented the cleavage of PARP in PRRSV-infected cells in a dose-dependent manner. Cleaved PARP nearly disappeared at the highest concentration of PDTC and NAC and was hardly detectable in cells treated with RTN at all concentrations tested. Fig. 9B shows that antioxidant treatment after PRRSV infection significantly affected apoptosis induction by PRRSV. All three antioxidants suppressed DNA fragmentation in a dose-dependent manner. Notably 150 μM PDTC or 20 ng/ml RTN reduced the level of DNA fragmentation in PRRSV-infected cells to that of mock-infected cells. The results presented here suggested that apoptosis caused by PRRSV may involve oxidative stress induced by ROS production.

*PRRSV-infected cells also have features of necrosis*

Miller and Fox (2004) suggested a higher level of necrosis than apoptosis was induced by PRRSV in MARC-145 cells. They evaluated necrosis by measuring DNA fragments released
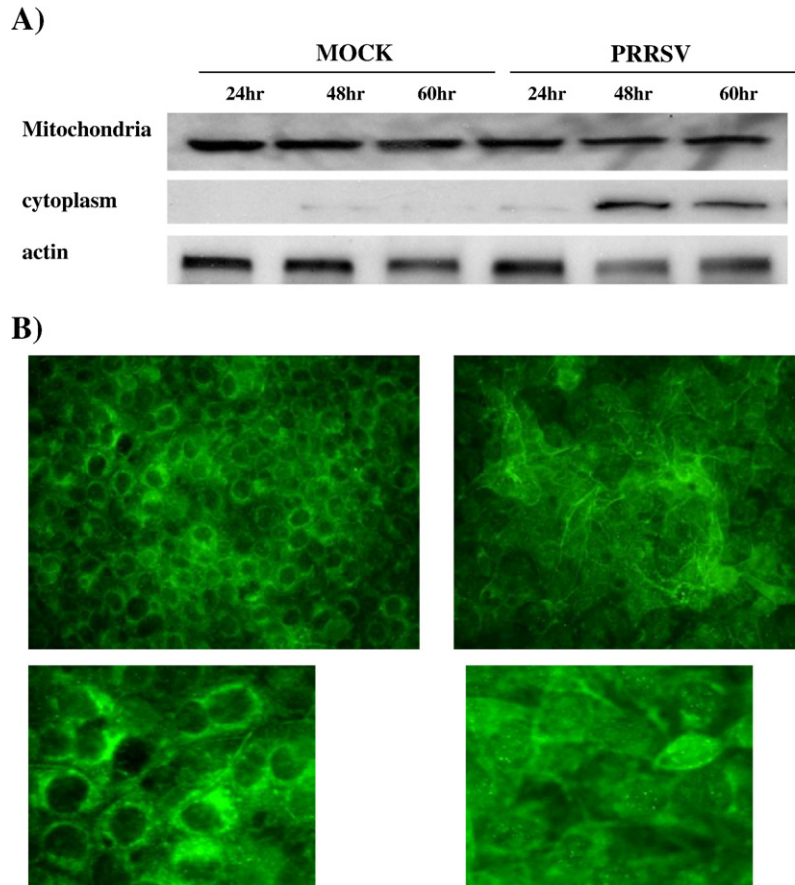
**A)**



**B)**



Fig. 8. PRRSV causes the release of cytochrome *c* from mitochondria. (A) The level of cytochrome *c* in mitochondria and cytoplasm was monitored by immunoblotting of mitochondrial extracts and cytoplasmic extracts from both adherent and floating cells. (B) Cytochrome *c* was visualized by IFA using monoclonal antibody specific for cytochrome *c*. These results are representative of two independent experiments.

from cells to cell culture medium. We determined if PRRSV-infected cells show necrotic characteristics as well as apoptosis. Cell culture supernatants from the same experiments analyzed for DNA fragmentation (see above) were used for necrosis detection. At 48 and 60 h p.i., a clear increase in DNA fragmentation in cell culture medium was detected in PRRSV-infected cells, indicating the presence of necrosis (Fig. 10A). Recently a specific necrosis factor has been identified. High mobility group 1 (HMGB1) protein is a chromatin-binding factor. When cellular membrane integrity is lost due to necrosis, HMGB1 translocates from nucleus to cytoplasm and then is rapidly released in to the extracellular space, resulting in inflammation and tissue damage (Andersson and Tracey, 2004; Bustin, 2002; Rovere-Querini et al., 2004). Therefore, to provide additional evidence for necrosis in PRRSV-infected cells, the level of this protein was monitored by immunoblotting. Fig. 10B shows that the level of HMGB1 in cytoplasm is slightly higher in PRRSV-infected cells than in corresponding control cells at 48 and 60 h p.i., implying that HMGB1 is released from cells. The release of HMGB1 from cells was further studied using flow cytometry analysis. When fixed and permeabilized cells were stained for HMGB1, a decrease in the fluorescence signal was found in PRRSV-infected cells, indicating that cell-associated HMGB1 is lost due to the release

of HMGB1 from necrotic cells (Fig. 10C). The effect of caspase inhibitor on necrosis was studied to determine if PRRSV-induced necrosis was secondary to apoptosis (Fig. 10D). With z-VAD-FMK treatment, the amount of DNA fragments released from PRRSV-infected cells was reduced from 1.57 to 1.06 at 100 μM and to 0.80 fold at 200 μM, compared to mock-infected cells, indicating that the release of DNA fragments from cells could be a secondary effect to apoptosis. These findings indicate that PRRSV may cause both forms of cell death, apoptosis and necrosis, in MARC-145 cells.

## Discussion

Previous studies have reported that apoptosis occurs in response to PRRSV infection of MARC-145 cells, PAM cultures, and pigs. These studies have characterized apoptosis mainly by morphological changes and DNA fragmentation analysis. In the present study, biochemical characteristics as well as morphological changes have been investigated to elucidate possible mechanisms involved in apoptosis of PRRSV-infected cells. We have shown that PRRSV-infected cells have characteristics of early and late apoptosis, namely PS exposure and chromatin condensation with DNA fragmentation, respectively. In addition, total caspase activity was signi-
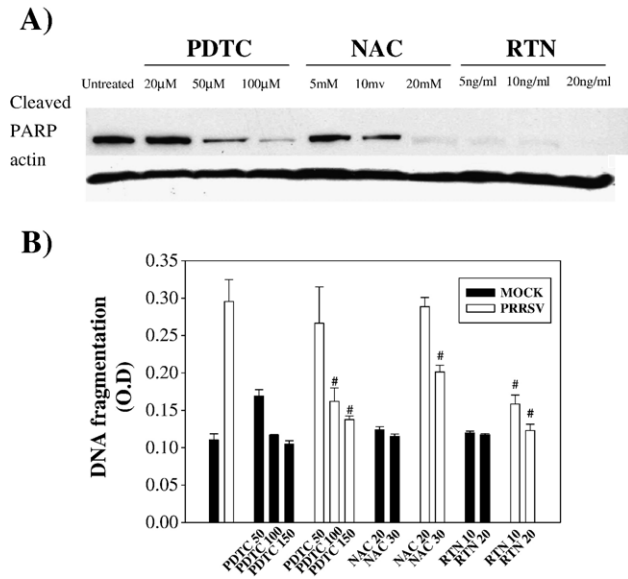
Fig. 9. Antioxidants prevented PARP cleavage caused by PRRSV. Cells were either mock-infected or infected with PRRSV and then treated with PDTC, NAC, and RTN at the indicated concentrations. (A) After 60 h induction, adherent cells were harvested by trypsin treatment and combined with floating cells. Whole cell extracts were prepared and then immunoblotted with a monoclonal antibody specific for cleaved PARP. A representative blot from three independent experiments is shown. (B) At 60 h p.i. the DNA fragmentation ELISA was performed with samples from triplicate wells. The ELISA was preformed in duplicate and values are shown as mean±SD. All experiments were repeated at least two times with similar results. #; $P < 0.001$ compared to untreated PRRSV-infected cells.

ficantly increased in PRRSV-infected cells and cleavage of a major caspase substrate, PARP, provided additional evidence for caspase activation. Many viruses trigger the activation of the caspase cascades, which in turn are responsible for apoptosis induction in virus-infected cells. To investigate the contribution of caspases to PRRSV-induced apoptosis, cells infected with PRRSV were treated with a broad spectrum caspase inhibitor. This caspase inhibitor significantly suppressed PARP cleavage as well as DNA fragmentation, suggesting that PRRSV-induced apoptosis is also a caspase-mediated process as seen in other viruses, including transmissible gastroenteritis virus and infectious bronchitis virus (Bartz and Emerman, 1999; Carthy et al., 1998; Devireddy and Jones, 1999; Eleouet et al., 1998; Galvan et al., 2000; Liu et al., 2001; Nava et al., 1998).

Caspase-dependent apoptosis can be initiated by extrinsic and intrinsic pathways, which are characterized by caspase-8 and caspase-9 activation, respectively. Numerous studies have demonstrated that viruses also use either extrinsic or intrinsic pathways, or both, to induce apoptosis. Viruses such as HIV, Lyssavirus, Tula hantavirus, sendai virus, and influenza virus induce apoptosis via caspase-8 mediated extrinsic pathway (Bartz and Emerman, 1999; Bitzer et al., 1999; Kassis et al., 2004; Li et al., 2004; Zhirnov et al., 2002). Intrinsic pathway activity via caspase-9 activation mediates apoptosis in VSV, rhinovirus, and parvovirus B19 (Deszcz et al., 2005; Gadaleta et al., 2005; Poole et al., 2004). In PRRSV infection, both caspases were activated. Caspase-8 and -9 could be activated indepen-

dently or caspase-9 activation could be the result of caspase-8 activation. The potential crosstalk between extrinsic and intrinsic pathways was proven by the dependency of caspase-9 activation on caspase-8 activity and the cleavage of Bid in PRRSV-infected cells. Similar results have been demonstrated for BVDV and hepatitis C virus (Chou et al., 2005; St-Louis et al., 2005).

Binding of a specific death ligand to the death receptor results in immediate recruitment of adaptor molecules such as Fas-associated death domain (FADD) and TNFR-associated death domain (TRADD), which interact with procaspase-8 to form a death inducing signaling complex (DISC). DISC triggers caspase-8 activation (Ashkenazi and Dixit, 1998). Caspase-8 activation by PRRSV implicated the involvement of a specific death receptor. Following PRRSV infection, TNFR1 and FasL expression on the cell surface was notably increased while Trail expression was slightly changed. This finding indicates that caspase-8 activation in PRRSV-infected cells could be mediated by ligation of TNFR1 and TNF-α, and Fas and FasL. Increased FasL expression was also detected on PRRSV-infected macrophages and caused apoptosis in co-cultured swine splenic lymphocytes (Chang et al., 2007). Future studies will determine the role of TNFR1 and FasL in PRRSV-induced apoptosis by using decoy receptors and neutralizing antibodies.

The Bcl-2 family includes both anti-apoptotic proteins such as Bcl-2, Bcl-XL Bcl-w, and Mcl-1 and pro-apoptotic proteins such as Bax, Bak, Bcl-Xs, Bid, Bad, and Bim/bod. In normal cells, apoptosis is inhibited by Bcl-2 which inactivates Bax by interacting and forming heterodimers. Pro-apoptotic signals induce translocation of Bax specifically to the mitochondria and Bax together with Bak form membrane-integrated homo-oligomers, which permeabilize the outer mitochondrial membrane and trigger a loss of the inner mitochondrial transmembrane potential ($\Delta\psi_m$) followed by the release of apoptotic factors such as cytochrome $c$ from the mitochondria to the cytoplasm. Therefore, the Bcl-2 family proteins have been considered as pivotal players in apoptosis, especially mitochondria-mediated apoptosis. Not surprisingly, viruses target these proteins to induce or inhibit apoptosis. Our study showed that PRRSV infection down-regulated Bcl-2 but upregulated Bax expression. Activation of Bax could be the result of cleavage of Bid by caspase-8 which generates tBid. Then tBid induces oligomerization of BAK and BAX, thereby inducing release of cytochrome $c$ (Wei et al., 2001). Upregulation of Bax/Bcl-2 expression ratio is also a mechanism by which SARS coronavirus and Bovine herpesvirus (VP22 protein) induce mitochondria-mediated apoptosis (Qiu et al., 2005; Ren et al., 2005). Over-expression of Bcl-2 has been shown to inhibit the intrinsic apoptosis pathway mediated by mitochondria. However, previous studies demonstrated that apoptosis induced by a recombinant vaccinia virus expressing GP5 of PRRSV was not prevented by Bcl-2 expression (Suarez et al., 1996). Despite this result, it is not clear whether PRRSV-induced apoptosis is independent of Bcl-2 expression because this previous study did not determine the effect of Bcl-2 over-expression on apoptosis induced by PRRSV infection and a PRRSV-nonpermissive N2A neuroblastoma cell line was used.
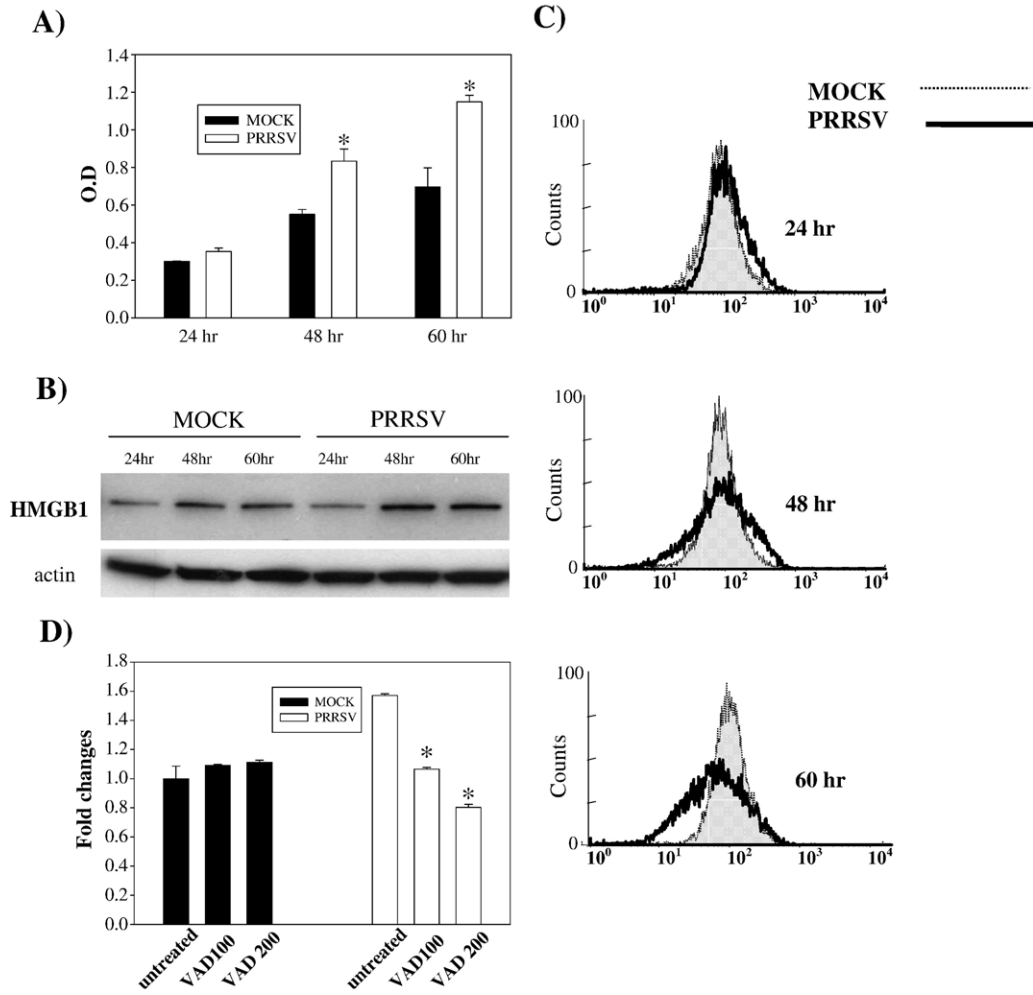
Fig. 10. PRRSV-infected cells show characteristics of necrosis. (A) The amount of DNA fragmentation in the cell culture medium was determined at the indicated time points using a DNA fragmentation ELISA. The ELISA was performed in duplicate and values are shown as mean±SD. These results are representative of three independent experiments. *; $P<0.001$ compared to mock-infected cells at the same point. (B) Cytoplasmic extracts from mock- or PRRSV-infected cells (both adherent and floating cells) were immunoblotted with polyclonal anti-HMGB1 antibody. HMGB1 protein was identified as a 29 kDa band. (C) Both adherent and floating cells were collected and fixed with 4% PFA followed by permeabilization with ice-cold ethanol. Cells were incubated with polyclonal anti-HMGB1 antibody followed by a secondary antibody conjugated with FITC. Cell-associated HMGB1 in cells was analyzed by flow cytometry. (D) Following infection, cells were treated with z-VAD-FMK and a DNA fragmentation ELISA was performed with cell culture supernatants from the indicated time points p.i. These results are representative of three independent experiments. *; $P<0.001$ compared to untreated PRRSV-infected cells.

Various pro-apoptotic signals converge on mitochondria, and the subsequent mitochondrial membrane permeabilization due to disruption of mitochondria transmembrane potential is a key event in the intrinsic apoptosis pathway. As expected from caspase-9 activation and increased Bax expression, PRRSV infection significantly disrupted mitochondria transmembrane potential and resulted in release of cytochrome $c$ from mitochondria into the cytoplasm. The released cytochrome $c$ forms an apoptosome consisting of Apaf-1 oligomers and adenine nucleotides (ATP) (Budihardjo et al., 1999; Chu et al., 2001). This apoptosome recruits caspase-9 to the complex and activates caspase-9 which in turn activates the executioner caspases, caspase-3 and caspase-7. Some viral proteins are known to be localized to mitochondria and induce apoptosis by altering mitochondrial function (Ciminale et al., 1999; Jacotot et al., 2000; Liu et al., 2002; Nudson et al., 2003). It is not known

whether PRRSV encodes a protein which directly targets mitochondria, resulting in apoptosis.

Apoptosis can be triggered in virus-infected cells as either a host defense mechanism or as a viral strategy to enhance viral replication and progeny virus production, avoidance of an immune response, and/or induction of persistent infection. Therefore, the role of apoptosis in PRRSV progeny release was studied here. Although PARP cleavage and DNA fragmentation in PRRSV-infected cells were blocked, comparable amounts of infectious virus were released from caspase-inhibitor-treated cells. These findings suggested that apoptosis is not required for the replication of PRRSV as shown in SARS coronavirus, infectious bronchitis virus, reovirus, and sendai virus, bovine herpesvirus type 4 (Bitzer et al., 1999; Bordi et al., 2006; Liu et al., 2001; Pagnini et al., 2004; Rodgers et al., 1997). Although apoptosis is an end-stage process and does not play an

important role in PRRSV replication *in vitro*, this does not exclude the possibility that apoptosis has an important contribution to PRRSV pathogenesis *in vivo*. In reovirus infection of mice, apoptosis is a major mechanism of reovirus-induced tissue injury (Clarke et al., 2005). It is also possible that PRRSV initially suppresses apoptotic pathways to maximize viral replication, but then at later times post-infection induces apoptosis to avoid an immune response and/or induce persistent infection.

Oxidative stress caused by ROS, including superoxide ($O_2^-$) and hydrogen peroxide ($H_2O_2$), has been suggested as an apoptosis mediator in virus-infected cells (Lowy and Dimitrov, 1997; Schweizer and Peterhans, 1999). Our previous study showed that PRRSV infection induced oxidative stress via ROS production in MARC-145 cells (Lee and Kleiboeker, 2005). Because ROS is known to activate the intrinsic pathway of apoptosis mediated by cytochrome *c* and caspase-9 (Chen et al., 2003), we determined if ROS produced by PRRSV was involved in inducing apoptosis. Treatments with three anti-oxidants (PDTC, NAC, and rotenone) protected cells from PRRSV-induced apoptosis, suggesting that oxidative stress may play a role in intrinsic apoptosis induction by PRRSV. Mitochondria are a major source of ROS and rotenone is a specific inhibitor of mitochondrial superoxide generation. Thus the anti-apoptotic effect of rotenone on PRRSV-infected cells indicates that mitochondrial-derived ROS may be involved in PRRSV-induced apoptosis. Oxidative stress induced by oxygen radicals and nitric oxide (NO) is a key event in the pathogenesis of various infectious diseases. For example, oxidative stress in chronic hepatitis C virus infection interferes with antiviral innate immune responses and exacerbates lung injury (Wang and Weinman, 2006). Tissue injury by oxidative stress is also associated with encephalitis caused by herpes simplex virus type 1 and reovirus, dementia caused by human immunodeficiency virus, and subacute sclerosing panencephalitis caused by measles virus (Steiner et al., 2006; Valyi-Nagy and Dermody, 2005). In addition to tissue injury, recent studies revealed that NO-induced oxidative stress accelerates viral mutation which may increase the heterogeneity of RNA viruses and lead to viral evolution under selective pressures (Akaike, 2001). It is possible that a cellular oxidative stress caused by ROS production plays a central role in PRRSV-induced apoptosis/necrosis and is involved in PRRSV pathogenesis based upon our findings. However, further studies are needed to determine mechanism(s) by which PRRSV induces oxidative stress, the viral protein(s) responsible for oxidative stress, and the role of oxidative stress in PRRSV pathogenesis *in vivo*.

In necrotic cells, DNA fragments as well as HMGB1 are released due to the loss of membrane integrity. These characteristics of necrosis were detected in PRRSV-infected cells. The observation that caspase inhibitor, z-VAD-FMK, reduced the amount of fragmented DNA released from PRRSV-infected cells indicates that caspase-dependent apoptosis induced by PRRSV could be followed by secondary necrosis. Apoptotic cells are removed by phagocytosis *in vivo*, but *in vitro* apoptotic cells undergo secondary necrosis in which the apoptotic bodies swell and eventually lyse (Wu et al., 2001). A

study has shown that PRRSV induces apoptosis followed by a necrotic-like cell death at later times p.i. Characteristics of late apoptosis such as nuclear condensation, DNA laddering, and terminal deoxynucleotidyl transferase (TdT)-mediated dUTP nick end-labeling (TUNEL) staining were only detected in unattached PRRSV-infected cells which were dead (Kim et al., 2002). This result provides additional evidence of necrosis secondary to apoptosis induction in PRRSV-infected cells although there is some disagreement with the present study. Other studies demonstrated that PRRSV leads to cell death by both apoptosis and necrosis mechanisms in MARC-145 cells and pig monocyte-derived dendritic cells (Miller and Fox, 2004; Wang et al., 2007).

Although more than 80% of cells were infected with PRRSV at 48 and 60 h p.i., not all cells were positive for total activated caspases as an apoptotic marker. This could be explained by several reasons. Most likely, the cells could be in different stages of viral infection due to the relatively low MOI used in the present study. In other words, there could be some cells in early stages of viral replication; therefore, apoptotic signals were too weak to be detected by the method used. In addition, cells that were necrotic secondary to apoptosis could explain cells unstained for active caspases but stained for viral protein.

The present study and previous studies agree that PRRSV induces apoptosis. However, it is still controversial whether PRRSV induces apoptosis directly in infected cells or indirectly in uninfected bystander cells via inflammatory cytokines. Discrepancies among these studies could be explained by several factors including different cell types, a fibroblast cell line versus immune cells which are able to produce high level of cytokines, *in vitro* versus *in vivo* infection, and the techniques used to measure apoptosis. Previous studies used DNA fragmentation as an apoptosis marker, which cannot detect cells in early stages of apoptosis. Therefore, if most PRRSV-infected cells were in early apoptosis process, those cells would not be detectable by the TUNEL assay. Our study showed that a majority of apoptotic cells were characterized by both early and late apoptosis markers and were PRRSV-infected. Apoptosis was evident at 48 h and 60 h post-infection when a majority of cells (approximately 90%) became positive for PRRSV infection. Therefore, most cells undergoing apoptosis are PRRSV-infected cells rather than uninfected bystander cells. The possible involvement of a bystander effect was also indicated by increased surface expression FasL on PRRSV-infected cells.

In summary, the present study demonstrated that (i) PRRSV infection causes characteristic morphological and biochemical changes of apoptosis such as chromatin condensation, DNA fragmentation, externalization of PS, caspase activation, and PARP cleavage; (ii) PRRSV induces caspase-dependent apoptosis and activates both caspase-8 and caspase-9; (iii) caspase-8 activated through ligation of the death ligand with the death receptor, possibly TNR-α/TNFR1 and Fas/FasL, mediates caspase-9 activation via Bid cleavage; (iv) PRRSV caused an increased ratio of Bax/Bcl-2 which is followed by the disruption of the mitochondrial transmembrane potential and cytochrome *c* release; (v) oxidative stress induced by PRRSV is

involved in apoptosis; and (vi) PRRSV infection causes secondary necrosis. Based on our findings, a schematic model of PRRSV-induced apoptosis mechanisms is suggested, as shown in Fig. 11. This is the first comprehensive study demonstrating mechanisms by which PRRSV induces apoptosis. However, the relevance of apoptosis during PRRSV infection *in vivo* remains to be determined. To understand the role of apoptosis in PRRSV pathogenesis, further studies will define the steps involved in the apoptotic signal transduction cascade and the interaction of viral components and cellular factors in PRRSV-infected cells. In addition, infectious cDNA clones will be useful to study the role of apoptosis in PRRSV pathogenesis since related PRRSV isolates of differing virulence can be compared based on their ability to induce apoptosis *in vitro* and *in vivo*.

## Materials and methods

### Cells and virus

The MARC-145 cell line, which is a clone of the African green monkey kidney cell line MA-104, and the HEK-293 cell line, which is derived from human embryonic kidney cells, were cultured and maintained in Dulbecco's Modified Eagle medium (DMEM) supplemented with 10% FBS, 0.25 μg/ml fungizone, 100 U/ml penicillin, 10 μg/ml streptomycin sulfate and 5 μg/ml gentamicin (BioWhittaker Inc., Walkersville, MD) and then held at 37 °C in a humidified 5% $CO_2$ incubator.

PRRSV isolate 25544 was obtained from clinical cases submitted to the University of Missouri's Veterinary Medicine Diagnostic Laboratory. Virus stocks of PRRSV were prepared in MARC-145 cells and infectious virus titers were analyzed in MARC-145 cells using the Reed and Muench method (Reed and Muench, 1938). A low multiplicity of infection (MOI <0.05) was used to prepare viral stocks. For virus infection, cells were initially adsorbed with virus at the indicated MOI for 1 h at 37 °C. After 1 h of adsorption, cells were gently washed with medium.



Fig. 11. Schematic representation of PRRSV-induced apoptosis pathways.

### Cell viability assay

Adherent cells were collected at different time points of infection by treatment with a solution of 0.25% trypsin–1 mM EDTA and were combined with the floating cells collected from the culture medium. Cell viability was determined by the trypan blue dye exclusion assay, and cells were counted under a microscope by using a hemocytometer.

### Reagents

Caspase peptide inhibitors, z-VAD-FMK (Axxora Life Sciences, San Diego, CA), z-IETD-FMK (BD Pharmingen, San Diego, CA), z-LEHD-FMK (BD Pharmingen, San Diego, CA), and z-DEVD-FMK (BD Pharmingen, San Diego, CA) were used to inhibit caspase activity. Stock solutions were prepared with DMSO and stored at −20 °C.

### Propidium iodide (PI) staining

Cells grown on chamber slides were fixed with ice-cold methanol for 20 min at 4 °C. Cells were washed with PBS three times and stained with 10 μg/ml PI and 100 μg/ml RNase (Sigma, St. Louis, MO) in PBS. Then slides were observed under UV microscope.

### Annexin V staining

MARC cells were stained with annexin V by using the annexin V staining kit (Roche Applied Science, Indianapolis, IN) as per the manufacturer's instructions. Briefly, adherent cells were harvest by trypsin treatment and combined with floating cells. Cells were washed with PBS and were resuspended in 400 μl of binding buffer followed by addition of annexin. Cells were incubated at room temperature for 15 min, and then 500 μl of binding buffer was added. Annexin staining was quantified by flow cytometry analysis using Beckman Coulter Cytomics FAScan cytometer using the FITC channel.

### Caspase activity assay

Caspase activity was measured using CaspGLOW Fluorescein Active Caspase Staining Kit (Bio Vision, Mountain View, CA). Adherent and floating cells were collected at the different time points of infection and centrifuged for 5 min at $400 \times g$. Cells were incubated at 37 °C for 40 min with a caspase family inhibitor VAD-FMK conjugated to FITC (FITC-VAD-FMK) which irreversibly binds to activated caspases in apoptotic cells. Cells were then washed with washing buffer and activated caspases in apoptotic cells were detected by a Beckman Coulter Cytomics FAScan cytometer using the FITC channel.

Quantification of caspase-8, -9, and -3 activity was measured by a colorimetric assay kit for each caspase (Bio Vision, Mountain View, CA). Activated caspases cleave the synthetic peptide substrates labeled with pNA to release free pNA, which is then quantified using spectrophotometer. Adherent and floating cells were collected and lysed on ice for 10 min. Cells were
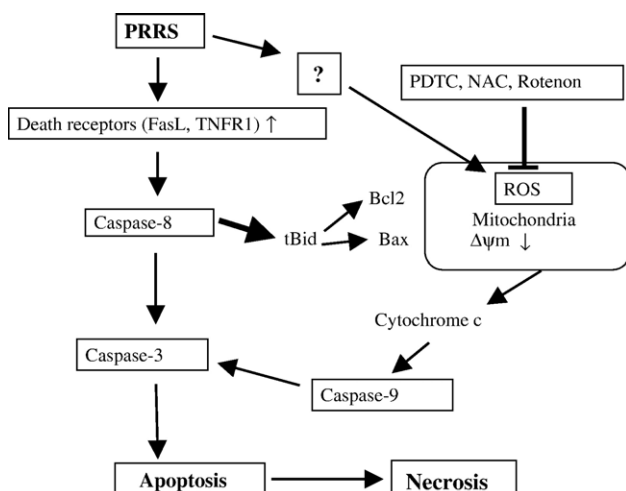
centrifuged for 1 min at 10,000×g and supernatants containing cytosolic extracts were assayed for protein concentration. One hundred micrograms of protein from each sample was incubated with caspase specific substrates, IETD-pNA (caspase-8), LEHD-pNA (caspase-9), and DEVD-pNA (caspase-3), for 2 h at 37 °C. Samples were read at 405 nm in spectrophotometer.

*Immunofluorescence antibody staining*

For TNFR1, Trail, FasL and cytochrome *c* immunofluorescent staining, cells grown on chamber slide were fixed with 10% paraformaldehyde (Polyscience, Warrington, PA) in PBS for 15 min on ice. Cells were then washed three times with PBS and incubated with primary antibody for 2 h at 37 °C followed by FITC-conjugated anti-rabbit IgG. After washing three times with PBS, slides were dried and mounted in Vectashield antifade media (Vector Laboratories, Burlingame, CA).

For Bax and Bcl-2, cells grown on chamber slides were fixed with 4% paraformaldehyde in PBS for 20 min on ice. Cell were then washed two times with PBS and permeabilized with 70% ethanol at −20 °C, followed by incubation with primary antibodies and secondary antibodies. After washing three times with PBS, slides were dried and mounted in Vectashield antifade media (Vector Laboratories, Burlingame, CA).

*Cellular DNA fragmentation ELISA*

DNA fragmentation was quantitatively measured using a cellular DNA fragmentation ELISA kit (Roche applied science, Indianapolis, IN) which detects BrdU-labeled DNA fragments in the cytoplasm for apoptosis and cell culture medium for necrosis. Briefly, cells were labeled with 10 μM BrdU for 24 h. After PRRSV infection, adherent and floating cells were collected and lysed with incubation buffer for 30 min at room temperature. Cell lysate and cell culture supernatant from each well were used to quantify DNA fragmentation. The DNA fragments were detected immunologically by the ELISA using two antibodies, an anti-DNA antibody and an anti-BrdU antibody peroxidase conjugate. The degree of apoptosis (cytosolic DNA fragments) and early necrosis (DNA released into the medium) was quantified. Samples were added into the well of 96 well plates coated with anti-DNA antibody. After incubation for 90 min at room temperature, the samples were denatured and fixed by microwave (500 W) for 5 min followed by a second 90 min incubation with peroxidase-conjugated anti-BrdU at room temperature. Substrate solution was then added and the reaction was stopped by the addition of 100 μl of 4 N HCl to each well. The absorbance was measured at 450 nm. All experiments were performed in triplicate wells and ELISA was done in duplicated wells. Therefore, values shown in the graphs are average from total of 6 ELISA measurements.

*Preparation of whole cell extracts and cytoplasmic and nuclear fractions*

For whole cell extracts, cells were collected by scraping directly into the medium, rinsed once with cold PBS, transferred to a 1.5-ml Eppendorf tube, and lysed in cell lysis buffer containing 20 mM Tris–HCl (pH 7.5), 150 mM NaCl, 1 mM Na$_2$EDTA, 1 mM EGTA, 1% Triton, 2.5 mM sodium pyrophosphate, 1 mM beta-glycerophosphate, 1 mM Na$_3$VO$_4$, and 1 μg/ml leupeptin. Samples were kept on ice for at least 10 min and centrifuged at 10,000×g for 20 min. Supernatants were stored at −80 °C.

Cytoplasmic and nuclear protein extracts from MARC-145 cells were prepared with the nuclear extraction kit (Active Motif, Inc., Carlsbad, CA) according to the manufacturer's protocol. Briefly, cells were collected by scraping directly into the medium, rinsed once with 1 ml ice-cold PBS/phosphatase inhibitors. Then cells were lysed with hypotonic lysis buffer for 15 min on ice and vortexed for 10 s after the addition of detergent. Samples were centrifuged at 1400×g for 30 s at 4 °C. The supernatant, cytoplasmic extract, was stored at −80 °C. The nuclear pellets were lysed with complete lysis buffer containing protease inhibitors and kept on ice for 30 min. Samples were vortexed vigorously for 30 s and centrifuged for 10 min at 4 °C. The supernatants and nuclear extracts were stored at −80 °C. Protein concentrations were determined by the Bio-Rad protein assay (Bio-Rad, Hercules, CA) with bovine serum albumin (BSA) as the standard.

*Mitochondrion purification and cytochrome c release*

Cytochrome *c* release from mitochondria into cytoplasm was monitored by Western blotting of both mitochondrial and cytoplasmic extracts (Bio Vision, Mountain View, CA). Mitochondria from adherent and floating cells were purified as described in manufacturer's manual with some modifications. Briefly, cells were resuspended with cytosol extraction buffer mix containing DTT and protease inhibitors then incubated on ice for 10 min. Cells were then homogenized and the homogenates were centrifuged 700×g for 10 min at 4 °C to remove nuclei, cellular debris, and intact cells. The supernatant containing the cytosol, including the mitochondria, was centrifuged at 10,000×g for 30 min at 4 °C. Supernatant was collected as the cytosolic fraction and the pellet was resuspended in mitochondrial extraction buffer mix containing DTT and protease inhibitors (prepared as described in the manufacturer's instructions) and saved as the mitochondrial fraction.

The cytosolic fraction was centrifuged again 10,000×g for at least 30 min at 4 °C to remove any residual mitochondria. The protein concentration of each fraction was measured using the Bio-Rad assay (Bio-Rad, Hercules, CA) with a BSA standard curve.

*MitoCapture assay*

Adherent and floating cells were collected at the different time points of infection and centrifuged for 5 min at 400×g. Then cells were washed once with PBS and the mitochondrial membrane potential was measured using the MitoCapture Kit (BioVision, Mountain View, CA). Briefly, cells were suspended in 1 ml of diluted MitoCapture reagent and incubated at 37 °C for 15 min. After centrifuging at 400×g for 5 min, the pellet was

suspended in 0.5 ml of pre-warmed MitoCapture buffer. MitoCapture-labeled cells were analyzed using a Beckman Coulter Cytomics FAScan cytometer using the FITC channel.

## Western blotting

Western blotting was performed by utilizing a standard protocol (Davis et al., 1994). Briefly, whole cell, cytoplasmic, or nuclear extracts were diluted (2:1) in 2× sample buffer and boiled for 5 min. Fifty micrograms of each extract was subjected to sodium dodecyl sulfate–polyacrylamide gel electrophoresis (SDS–PAGE) and transferred to a nitrocellulose membrane (Amersham Biosciences, Piscataway, NJ). The membrane was washed with phosphate-buffered saline–Tween 20 (TPBS), blocked in a solution of TPBS containing 5% nonfat dry milk, and then washed three times. The membrane was incubated with primary antibody overnight at 4 °C or 1 h at RT, washed three times with TPBS, and incubated with the secondary antibody horseradish peroxidase (HRP) conjugate solution for 1 h at RT. Samples were washed three times with TPBS, and the signal was detected with a chemiluminescent protein detection system (Amersham Biosciences, Piscataway, NJ). Antibodies used for Western blot were anti-Trail, anti-TNFR1, anti-FasL, and anti-Bid (Santa Cruz Biotechnology, Santa Cruz, CA), Bcl-2, and Bax (Cell Signaling, Beverly, MA), anti-rabbit IgG-HRP and anti-mouse IgG-HRP (Amersham Biosciences, Piscataway, NJ), and anti-actin (Sigma, St. Louis, MO).

## Statistical analysis

The Student's t-test was used for the statistical analyses. P-values less than 0.05 were considered statistically significant.

## Acknowledgments

## References

Akaike, T., 2001. Role of free radicals in viral pathogenesis and mutation. Rev. Med. Virol. 11 (2), 87–101.

Andersson, U., Tracey, K.J., 2004. HMGB1 as a mediator of necrosis-induced inflammation and a therapeutic target in arthritis. Rheum. Dis. Clin. North Am. 30 (3), 627–637 (xi).

Ashkenazi, A., Dixit, V.M., 1998. Death receptors: signaling and modulation. Science 281 (5381), 1305–1308.

Bartz, S.R., Emerman, M., 1999. Human immunodeficiency virus type 1 Tat induces apoptosis and increases sensitivity to apoptotic signals by up-regulating FLICE/caspase-8. J. Virol. 73 (3), 1956–1963.

Bitzer, M., Prinz, F., Bauer, M., Spiegel, M., Neubert, W.J., Gregor, M., Schulze-Osthoff, K., Lauer, U., 1999. Sendai virus infection induces apoptosis through activation of caspase-8 (FLICE) and caspase-3 (CPP32). J. Virol. 73 (1), 702–708.

Bordi, L., Castilletti, C., Falasca, L., Ciccosanti, F., Calcaterra, S., Rozera, G., Di Caro, A., Zaniratti, S., Rinaldi, A., Ippolito, G., Piacentini, M., Capobianchi, M.R., 2006. Bcl-2 inhibits the caspase-dependent apoptosis induced by SARS-CoV without affecting virus replication kinetics. Arch. Virol. 151 (2), 369–377.

Budihardjo, I., Oliver, H., Lutter, M., Luo, X., Wang, X., 1999. Biochemical pathways of caspase activation during apoptosis. Annu. Rev. Cell Dev. Biol. 15, 269–290.

Bustin, M., 2002. At the crossroads of necrosis and apoptosis: signaling to multiple cellular targets by HMGB1. Sci. STKE 2002 (151), E39.

Carthy, C.M., Granville, D.J., Watson, K.A., Anderson, D.R., Wilson, J.E., Yang, D., Hunt, D.W., McManus, B.M., 1998. Caspase activation and specific cleavage of substrates after coxsackievirus B3-induced cytopathic effect in HeLa cells. J. Virol. 72 (9), 7669–7675.

Chang, H.W., Jeng, C.R., Liu, J.J., Lin, T.L., Chang, C.C., Chia, M.Y., Tsai, Y.C., Pang, V.F., 2005. Reduction of porcine reproductive and respiratory syndrome virus (PRRSV) infection in swine alveolar macrophages by porcine circovirus 2 (PCV2)-induced interferon-alpha. Vet. Microbiol. 108 (3–4), 167–177.

Chang, H.W., Jeng, C.R., Lin, C.M., Liu, J.J., Chang, C.C., Tsai, Y.C., Chia, M.Y., Pang, V.F., 2007. The involvement of Fas/FasL interaction in porcine circovirus type 2 and porcine reproductive and respiratory syndrome virus co-inoculation-associated lymphocyte apoptosis in vitro. Vet. Microbiol.

Chen, Q., Chai, Y.C., Mazumder, S., Jiang, C., Macklis, R.M., Chisolm, G.M., Almasan, A., 2003. The late increase in intracellular free radical oxygen species during apoptosis is associated with cytochrome c release, caspase activation, and mitochondrial dysfunction. Cell Death Differ. 10 (3), 323–334.

Choi, C., Chae, C., 2002. Expression of tumour necrosis factor-alpha is associated with apoptosis in lungs of pigs experimentally infected with porcine reproductive and respiratory syndrome virus. Res. Vet. Sci. 72 (1), 45–49.

Chou, A.H., Tsai, H.F., Wu, Y.Y., Hu, C.Y., Hwang, L.H., Hsu, P.I., Hsu, P.N., 2005. Hepatitis C virus core protein modulates TRAIL-mediated apoptosis by enhancing Bid cleavage and activation of mitochondria apoptosis signaling pathway. J. Immunol. 174 (4), 2160–2166.

Chu, Z.L., Pio, F., Xie, Z., Welsh, K., Krajewska, M., Krajewski, S., Godzik, A., Reed, J.C., 2001. A novel enhancer of the Apaf1 apoptosome involved in cytochrome c-dependent caspase activation and apoptosis. J. Biol. Chem. 276 (12), 9239–9245.

Ciminale, V., Zotti, L., D'Agostino, D.M., Ferro, T., Casareto, L., Franchini, G., Bernardi, P., Chieco-Bianchi, L., 1999. Mitochondrial targeting of the p13II protein coded by the x-II ORF of human T-cell leukemia/lymphotropic virus type I (HTLV-I). Oncogene 18 (31), 4505–4514.

Clarke, P., Richardson-Burns, S.M., DeBiasi, R.L., Tyler, K.L., 2005. Mechanisms of apoptosis during reovirus infection. Curr. Top. Microbiol. Immunol. 289, 1–24.

Connolly, J.L., Rodgers, S.E., Clarke, P., Ballard, D.W., Kerr, L.D., Tyler, K.L., Dermody, T.S., 2000. Reovirus-induced apoptosis requires activation of transcription factor NF-kappaB. J. Virol. 74 (7), 2981–2989.

Cryns, V., Yuan, J., 1998. Proteases to die for. Genes Dev. 12 (11), 1551–1570.

Davis, L., Kuehl, M., Battey, J., 1994. Basic Methods in Molecular Biology. Appleton and Lange, Norwalk, CT.

Deszcz, L., Gaudernak, E., Kuechler, E., Seipelt, J., 2005. Apoptotic events induced by human rhinovirus infection. J. Gen. Virol. 86 (Pt. 5), 1379–1389.

Devireddy, L.R., Jones, C.J., 1999. Activation of caspases and p53 by bovine herpesvirus 1 infection results in programmed cell death and efficient virus release. J. Virol. 73 (5), 3778–3788.

Eleouet, J.F., Chilmonczyk, S., Besnardeau, L., Laude, H., 1998. Transmissible gastroenteritis coronavirus induces programmed cell death in infected cells through a caspase-dependent pathway. J. Virol. 72 (6), 4918–4924.

Everett, H., McFadden, G., 1999. Apoptosis: an innate immune response to virus infection. Trends Microbiol. 7 (4), 160–165.

Gadaleta, P., Perfetti, X., Mersich, S., Coulombie, F., 2005. Early activation of the mitochondrial apoptotic pathway in vesicular stomatitis virus-infected cells. Virus Res. 109 (1), 65–69.

Gagnon, C.A., Lachapelle, G., Langelier, Y., Massie, B., Dea, S., 2003. Adenoviral-expressed GP5 of porcine respiratory and reproductive syndrome virus differs in its cellular maturation from the authentic viral protein but maintains known biological functions. Arch. Virol. 148 (5), 951–972.

Galvan, V., Brandimarti, R., Munger, J., Roizman, B., 2000. Bcl-2 blocks a caspase-dependent pathway of apoptosis activated by herpes simplex virus 1 infection in HEp-2 cells. J. Virol. 74 (4), 1931–1938.

Jacotot, E., Ravagnan, L., Loeffler, M., Ferri, K.F., Vieira, H.L., Zamzami, N., Costantini, P., Druillennec, S., Hoebeke, J., Briand, J.P., Irinopoulou, T., Daugas, E., Susin, S.A., Cointe, D., Xie, Z.H., Reed, J.C., Roques, B.P., Kroemer, G., 2000. The HIV-1 viral protein R induces apoptosis via a direct effect on the mitochondrial permeability transition pore. J. Exp. Med. 191 (1), 33–46.

Kassis, R., Larrous, F., Estaquier, J., Bourhy, H., 2004. Lyssavirus matrix protein induces apoptosis by a TRAIL-dependent mechanism involving caspase-8 activation. J. Virol. 78 (12), 6543–6555.

Kidd, V.J., 1998. Proteolytic activities that mediate apoptosis. Annu. Rev. Physiol. 60, 533–573.

Kim, T.S., Benfield, D.A., Rowland, R.R., 2002. Porcine reproductive and respiratory syndrome virus-induced cell death exhibits features consistent with a nontypical form of apoptosis. Virus Res. 85 (2), 133–140.

Labarque, G., Van Gucht, S., Nauwynck, H., Van Reeth, K., Pensaert, M., 2003. Apoptosis in the lungs of pigs infected with porcine reproductive and respiratory syndrome virus and associations with the production of apoptogenic cytokines. Vet. Res. 34 (3), 249–260.

Lee, S.M., Kleiboeker, S.B., 2005. Porcine arterivirus activates the NF-kappaB pathway through IkappaB degradation. Virology 342 (1), 47–59.

Lee, C., Rogan, D., Erickson, L., Zhang, J., Yoo, D., 2004. Characterization of the porcine reproductive and respiratory syndrome virus glycoprotein 5 (GP5) in stably expressing cells. Virus Res. 104 (1), 33–38.

Li, H., Zhu, H., Xu, C.J., Yuan, J., 1998. Cleavage of BID by caspase 8 mediates the mitochondrial damage in the Fas pathway of apoptosis. Cell 94 (4), 491–501.

Li, X.D., Kukkonen, S., Vapalahti, O., Plyusnin, A., Lankinen, H., Vaheri, A., 2004. Tula hantavirus infection of Vero E6 cells induces apoptosis involving caspase 8 activation. J. Gen. Virol. 85 (Pt. 11), 3261–3268.

Liu, C., Xu, H.Y., Liu, D.X., 2001. Induction of caspase-dependent apoptosis in cultured cells by the avian coronavirus infectious bronchitis virus. J. Virol. 75 (14), 6402–6409.

Liu, J., Wei, T., Kwang, J., 2002. Avian encephalomyelitis virus induces apoptosis via major structural protein VP3. Virology 300 (1), 39–49.

Lowy, R.J., Dimitrov, D.S., 1997. Characterization of influenza virus-induced death of J774.1 macrophages. Exp. Cell Res. 234 (2), 249–258.

Miller, L.C., Fox, J.M., 2004. Apoptosis and porcine reproductive and respiratory syndrome virus. Vet. Immunol. Immunopathol. 102 (3), 131–142.

Nava, V.E., Rosen, A., Veliuona, M.A., Clem, R.J., Levine, B., Hardwick, J.M., 1998. Sindbis virus induces apoptosis through a caspase-dependent, CrmA-sensitive pathway. J. Virol. 72 (1), 452–459.

Nudson, W.A., Rovnak, J., Buechner, M., Quackenbush, S.L., 2003. Walleye dermal sarcoma virus Orf C is targeted to the mitochondria. J. Gen. Virol. 84 (Pt 2), 375–381.

Pagnini, U., Montagnaro, S., Pacelli, F., De Martino, L., Florio, S., Rocco, D., Iovane, G., Pacilio, M., Gabellini, C., Marsili, S., Giordano, A., 2004. The involvement of oxidative stress in bovine herpesvirus type 4-mediated apoptosis. Front Biosci. 9, 2106–2114.

Poole, B.D., Karetnyi, Y.V., Naides, S.J., 2004. Parvovirus B19-induced apoptosis of hepatocytes. J. Virol. 78 (14), 7775–7783.

Qiu, Z., Zhu, J., Harms, J.S., Friedrichsen, J., Splitter, G.A., 2005. Bovine herpesvirus VP22 induces apoptosis in neuroblastoma cells by upregulating the expression ratio of Bax to Bcl-2. Hum. Gene Ther. 16 (1), 101–108.

Reed, L.J., Muench, H.A., 1938. Method of determining fifty percent endpoints. Am. J. Hyg. 27, 494–497.

Ren, L., Yang, R., Guo, L., Qu, J., Wang, J., Hung, T., 2005. Apoptosis induced by the SARS-associated coronavirus in Vero cells is replication-dependent and involves caspase. DNA Cell Biol. 24 (8), 496–502.

Rodgers, S.E., Barton, E.S., Oberhaus, S.M., Pike, B., Gibson, C.A., Tyler, K.L.,

Dermody, T.S., 1997. Reovirus-induced apoptosis of MDCK cells is not linked to viral yield and is blocked by Bcl-2. J. Virol. 71 (3), 2540–2546.

Rovere-Querini, P., Capobianco, A., Scaffidi, P., Valentinis, B., Catalanotti, F., Giazzon, M., Dumitriu, I.E., Muller, S., Iannacone, M., Traversari, C., Bianchi, M.E., Manfredi, A.A., 2004. HMGB1 is an endogenous immune adjuvant released by necrotic cells. EMBO Rep. 5 (8), 825–830.

Roy, S., Nicholson, D.W., 2000. Cross-talk in cell death signaling. J. Exp. Med. 192 (8), F21–F25.

Rudin, C.M., Thompson, C.B., 1997. Apoptosis and disease: regulation and clinical relevance of programmed cell death. Annu. Rev. Med. 48, 267–281.

Schwartz, L.M., Smith, S.W., Jones, M.E., Osborne, B.A., 1993. Do all programmed cell deaths occur via apoptosis? Proc. Natl. Acad. Sci. U.S.A. 90 (3), 980–984.

Schweizer, M., Peterhans, E., 1999. Oxidative stress in cells infected with bovine viral diarrhoea virus: a crucial step in the induction of apoptosis. J. Gen. Virol. 80 (Pt 5), 1147–1155.

Sirinarumitr, T., Zhang, Y., Kluge, J.P., Halbur, P.G., Paul, P.S., 1998. A pneumo-virulent United States isolate of porcine reproductive and respiratory syndrome virus induces apoptosis in bystander cells both in vitro and in vivo. J. Gen. Virol. 79 (Pt. 12), 2989–2995.

St-Louis, M.C., Massie, B., Archambault, D., 2005. The bovine viral diarrhea virus (BVDV) NS3 protein, when expressed alone in mammalian cells, induces apoptosis which correlates with caspase-8 and caspase-9 activation. Vet. Res. 36 (2), 213–227.

Steiner, J., Haughey, N., Li, W., Venkatesan, A., Anderson, C., Reid, R., Malpica, T., Pocernich, C., Butterfield, D.A., Nath, A., 2006. Oxidative stress and therapeutic approaches in HIV dementia. Antioxid. Redox Signal. 8 (11–12), 2089–2100.

Suarez, P., Diaz-Guerra, M., Prieto, C., Esteban, M., Castro, J.M., Nieto, A., Ortin, J., 1996. Open reading frame 5 of porcine reproductive and respiratory syndrome virus as a cause of virus-induced apoptosis. J. Virol. 70 (5), 2876–2882.

Sur, J.H., Doster, A.R., Christian, J.S., Galeota, J.A., Wills, R.W., Zimmerman, J.J., Osorio, F.A., 1997. Porcine reproductive and respiratory syndrome virus replicates in testicular germ cells, alters spermatogenesis, and induces germ cell death by apoptosis. J. Virol. 71 (12), 9170–9179.

Sur, J.H., Doster, A.R., Osorio, F.A., 1998. Apoptosis induced in vivo during acute infection by porcine reproductive and respiratory syndrome virus. Vet. Pathol. 35 (6), 506–514.

Thomson, B.J., 2001. Viruses and apoptosis. Int. J. Exp. Pathol. 82 (2), 65–76.

Valyi-Nagy, T., Dermody, T.S., 2005. Role of oxidative damage in the pathogenesis of viral infections of the nervous system. Histol. Histopathol. 20 (3), 957–967.

Wang, T., Weinman, S.A., 2006. Causes and consequences of mitochondrial reactive oxygen species generation in hepatitis C. J. Gastroenterol. Hepatol. 21 (Suppl. 3), S34–S37.

Wang, X., Eaton, M., Mayer, M., Li, H., He, D., Nelson, E., Christopher-Hennings, J., 2007. Porcine reproductive and respiratory syndrome virus productively infects monocyte-derived dendritic cells and compromises their antigen-presenting ability. Arch. Virol. 152 (2), 289–303.

Wei, M.C., Zong, W.-X., Cheng, E.H.-Y., Lindsten, T., Panoutsakopoulou, V., Ross, A.J., Roth, K.A., MacGregor, G.R., Thompson, C.B., Korsmeyer, S.J., 2001. Proapoptotic BAX and BAK: a requisite gateway to mitochondrial dysfunction and death. Science 292 (5517), 727–730.

Wu, X., Molinaro, C., Johnson, N., Casiano, C.A., 2001. Secondary necrosis is a source of proteolytically modified forms of specific intracellular autoantigens: implications for systemic autoimmunity. Arthritis Rheum. 44 (11), 2642–2652.

Zhirnov, O.P., Ksenofontov, A.L., Kuzmina, S.G., Klenk, H.D., 2002. Interaction of influenza A virus M1 matrix protein with caspases. Biochemistry (Mosc) 67 (5), 534–539.